This is the accepted manuscript (postprint) of the following article:
E. Salahinejad, R. Amini, M. Marasi, M. J. Hadianfard, *Microstructure and wear behavior of a porous nanocrystalline nickel-free austenitic stainless steel developed by powder metallurgy*, Materials and Design 31 (2010) 2259–2263.
http://dx.doi.org/10.1016/j.matdes.2009.10.008

Microstructure and wear behavior of a porous nanocrystalline nickel-free austenitic stainless steel developed by powder metallurgy

E. Salahinejad [a,*], R. Amini [b], M. Marasi [a], M. J. Hadianfard [a]

[a] Department of Materials Science and Engineering, School of Engineering, Shiraz University, Zand Blvd, 7134851154, Shiraz, Iran

[b] Department of Materials Science and Engineering, Shiraz University of Technology, Modarres Blvd., 3619995161, Shiraz, Iran

Abstract

This paper investigates the microstructure and dry sliding wear characteristics of a porous Cr–Mn–N austenitic stainless steel prepared by powder metallurgy. The densification of the mechanically alloyed 18Cr–8Mn–0.9N stainless steel powder is performed by sintering at 1100 ºC for 20 h and subsequently water-quenching. This procedure gives rise to the development of a nanostructured austenitic stainless steel with a relative density of 85%. The porous biocompatible stainless steel exhibits an outstanding wear resistance compared with AISI 316L stainless steel samples. This is attributed to its considerable intrinsic hardness and its specific configuration of pores.

Keywords: Nano materials (A); Powder metallurgy (C); Wear (E)

* **Corresponding Author:** *Email address:* erfan.salahinejad@gmail.com (Erfan Salahinejad)

This is the accepted manuscript (postprint) of the following article:
E. Salahinejad, R. Amini, M. Marasi, M. J. Hadianfard, *Microstructure and wear behavior of a porous nanocrystalline nickel-free austenitic stainless steel developed by powder metallurgy*, Materials and Design 31 (2010) 2259–2263.
http://dx.doi.org/10.1016/j.matdes.2009.10.008

1. Introduction

In the recent years, nitrogen-alloyed nickel-free austenitic stainless steels have attracted a lot of attention. Their biocompatibility, superior mechanical properties, good corrosion resistance, and low costs make them attractive, particularly in biomedical applications [1–4]. On the other hand, nanostructured materials have recently developed into the subject of numerous researches, because of showing different properties compared to conventional coarse-grained materials [5]. It is well established that mechanical alloying (MA) is a promising method to synthesize nanostructures [6]. Moreover, MA under a nitrogen gas atmosphere results in the infusion of nitrogen into the structure of stainless steel powders, due to a solid-gas reaction [7–13]. Recently, studies on MA and some properties of Fe–Cr–Mn–N alloys powders have been reported [7–9].

In the biomedical field, porous materials with sufficient mechanical properties have been recognized as desired bone implants currently. The porous implants provide a better fixation of implants to the bone host, via the growth of new bone tissue into the pore spaces. Furthermore, introducing pores into stainless steel parts results in a decrease in the mismatch of elastic moduli of the implant and surrounding bone, thereby improving the fixation [10,14]. There are several reports in the literature on the fabrication of porous austenitic stainless steel biomaterials, for instance by MA and conventional sintering [10], selective laser sintering [14], and continuous zone melting under pressurized gases [2]. Moreover, Cui et al. [15] have conducted a study on the processing of high-nitrogen nickel-free austenitic stainless steels by powder injection molding, conventional sintering, and solid-nitriding, to achieve a relative density of 99 %. In addition, the same authors have reported the

This is the accepted manuscript (postprint) of the following article:
E. Salahinejad, R. Amini, M. Marasi, M. J. Hadianfard, *Microstructure and wear behavior of a porous nanocrystalline nickel-free austenitic stainless steel developed by powder metallurgy*, Materials and Design 31 (2010) 2259–2263.
http://dx.doi.org/10.1016/j.matdes.2009.10.008

development of porous nanocrystalline nitrogen-containing nickel-free austenitic stainless steels by powder metallurgy [10].

Because of relative movements between orthopedic implants, fixing screws, and surrounding bones [16], the wear resistance of a material being a candidate for biomedical applications is an essential property, which should be considered. Several attempts have been reported to improve the wear resistance of stainless steel implants, especially by using surface engineering approaches, including ion implantation and thin wear resistant coatings. Gradzka-Dahlke et al. [17] have pointed out an improvement in the wear resistance of porous 316L stainless steels compared to the non-porous components in lubricant conditions. Furthermore, it was frequently reported that the nitrogen addition to austenitic stainless steels increases the wear resistance [18–20]. Thomann and Uggowitzer [16] have reported that PANACEA P558 alloy, which is a high-nitrogen nickel-free austenitic stainless steel, presents a better wear resistance compared with 316L and Rex734.

In this study, the microstructure of high-nitrogen nickel-free austenitic stainless steel parts prepared from mechanically alloyed powders is assessed. Afterward, dry sliding wear characteristics of the produced parts are considered and also compared with those of AISI 316L stainless steel specimens.

2. Experimental procedure

2.1. Sample preparation and characterization

Fe–18Cr–8Mn–0.973N (wt.%) stainless steel powder was used as the primary material. Table 1 tabulates the exact composition of the powder, obtained from X-ray fluorescence (Philips PW2400) and LECO (Leco Corp., St. Joseph, MI) analyses. This powder was the

This is the accepted manuscript (postprint) of the following article:
E. Salahinejad, R. Amini, M. Marasi, M. J. Hadianfard, *Microstructure and wear behavior of a porous nanocrystalline nickel-free austenitic stainless steel developed by powder metallurgy*, Materials and Design 31 (2010) 2259–2263.
http://dx.doi.org/10.1016/j.matdes.2009.10.008

product of MA of 74Fe–18Cr–8Mn powder mixture under a nitrogen gas atmosphere, milled for 48 h. Details of the variables of the MA process are found in Ref. [7]. The as-milled powder consisted of 22.9 wt.% ferrite (α), 37.8 wt.% austenite (γ), and 39.3 wt.% an amorphous phase. In addition, the crystallite size of the α and γ phases was 14 and 11 nm, respectively [7].

The powder was uniaxially cold-pressed to cylinders at a compressive pressure of 1 GPa. The densification process was performed by sintering at 1100 ºC for 20 h and subsequently water-quenching to room temperature to achieve an austenitic structure. To prohibit the oxidation of the material during sintering, the compacts were encapsulated in quartz tubes under a vacuum condition. The density of the sintered sample was measured by Archimedes water immersion method. The theoretical density of the as-milled powder particles was measured as 7.705 g/cm3 by a pycnometer using He gas. It is mentioned that the sintering behavior of this alloy has been investigated by the same authors recently [10]. The corresponding results showed that sintering at 1100 ºC for 20 h leads to the maximum yield stress compared to that at the same temperature for other sintering times [10].

The resultant microstructure was studied by scanning electron microscopy (SEM, JEOL-JSM 5310), X-ray diffraction (XRD) (Shimadzu Lab X-6000 with Cu Kα radiation), and transmission electron microscopy (TEM, JEOL-JEM 2010). The quantitative analysis of the XRD data was performed by TOPAS 3 from Bruker AXS. By this software, the percentage of present phases was estimated by the Rietveld method and also the average crystallite size of crystalline phases was determined by the Double-Voigt approach. For TEM observations, the samples were first cut into discs of 3 mm diameter, manually ground to about 35 μm thickness, and then ion-milled at low temperatures. In addition, to determine the

This is the accepted manuscript (postprint) of the following article:
E. Salahinejad, R. Amini, M. Marasi, M. J. Hadianfard, *Microstructure and wear behavior of a porous nanocrystalline nickel-free austenitic stainless steel developed by powder metallurgy*, Materials and Design 31 (2010) 2259–2263.
http://dx.doi.org/10.1016/j.matdes.2009.10.008

nitrogen concentration changes after the consolidation, the LECO analysis was again employed.

2.2. Hardness and dry sliding wear tests

The Vickers micro-hardness at pore-free zones and the Vickers bulk hardness were measured on 10 points by applying 50 g and 31.25 kg loads, respectively and the average values are reported. The dry sliding behavior of the prepared nickel-free stainless steel was studied by means of a pin-on-disc tribometer at room temperature, according to ASTM standard G99. The wear tests were carried out in air without lubrication. 440C stainless steel pins with a hardness of 65 HRC and a diameter of 5 mm were employed as the counterface (slider). The sample discs were prepared with a diameter of 15 mm and thickness of 4 mm by the aforementioned densification process. Prior to the wear tests, the sample surface was metallographically polished with a paste containing diamond particles with a mean diameter of 1 μm. A load of 15 N, sliding speed of 0.06 ms^{-1}, and sliding distances of 200, 400, 600, and 800 m with a wear track diameter of 7 mm were conducted in the tests. For each individual sliding distance, a fresh disc was slid and then the weight change of the samples and the related pins was measured. In addition, the friction coefficient was in situ recorded and stored in a computer system by a strain gauge transducer. At least three replicates were performed for each sliding distance and the average value is reported. Finally, the worn surface was observed by SEM in order to identify the wear mechanism. To compare the wear resistance to a basis, the wear experiment was also conducted on wrought AISI 316L austenitic stainless steel samples with an average grain size of 10 μm.

This is the accepted manuscript (postprint) of the following article:
E. Salahinejad, R. Amini, M. Marasi, M. J. Hadianfard, *Microstructure and wear behavior of a porous nanocrystalline nickel-free austenitic stainless steel developed by powder metallurgy*, Materials and Design 31 (2010) 2259–2263.
http://dx.doi.org/10.1016/j.matdes.2009.10.008

3. Results and discussion

3.1. Structure of the sintered specimen

The relative density of the sintered samples was measured as 85%. It is noted that the presence of porosities is recognized to be suitable for some applications like biomaterials [14]. The SEM micrograph taken from the sintered specimen is given in Fig. 1, showing porosities exceeding 10 μm in size. As presented in Fig. 1, the primary powder particles can not be recognizable, suggesting that a tolerable necking is created between the primary powder particles.

The LECO analysis after the densification process depicts that the decrease in the nitrogen concentration, due to holding at the sintering temperature, is negligible (less than 0.03 wt.%). This is attributed to the small volume of the sealed quartz capsules. It suggests that the encapsulation technique is a very efficient route to preserve nitrogen during sintering of nitrogen-containing alloys.

The XRD pattern of the sintered samples is demonstrated in Fig. 2, illustrating a fully austenitic structure with a crystallite size of 90 nm. Since the γ phase has larger interstitial sites and smaller interfacial energy compared to the α phase [7], nitrogen which is interstitially dissolved in Fe-based alloys promotes the γ phase formation. However, it is well known that the microstructure of nitrogen-containing stainless steels depends on their nitrogen concentration and final heat treatment [11–13]. The XRD result demonstrated in Fig. 2 verifies that annealing at 1100 ºC and then water-quenching for this grade are an appropriate heat treatment cycle to develop an austenitic structure. Note that water-quenching from 1100 ºC prohibits the onset of diffusional phase transformations.

This is the accepted manuscript (postprint) of the following article:
E. Salahinejad, R. Amini, M. Marasi, M. J. Hadianfard, *Microstructure and wear behavior of a porous nanocrystalline nickel-free austenitic stainless steel developed by powder metallurgy*, Materials and Design 31 (2010) 2259–2263.
http://dx.doi.org/10.1016/j.matdes.2009.10.008

Fig. 3 depicts the TEM image and corresponding selected area diffraction (SAD) pattern of the sintered material. It can be seen that the microstructure is composed of the nanocrystalline γ phase, confirming the XRD results. It is noticeable that despite the relatively long sintering time, the crystallite size is still preserved in the nanometeric scale. That is, in spite of the fact that a rapid grain growth is anticipated at the sintering temperature, the material has shown a considerable thermal stability associated with an inherent resistance to grain growth. It is well known that the kinetics of grain growth is governed by grain boundary mobility. The main factors affecting grain boundary mobility in nanostructures are grain boundaries segregation, solute impurity, porosity, chemical ordering, and secondary phases [11]. In this study, the retarded grain growth causing the development of the nanostructure after sintering is attributed to [10]:

1. Segregation of nitrogen atoms toward grain boundaries: Since the solubility of nitrogen is limited in crystalline structures, nitrogen atoms tend to segregate toward grain boundaries to decrease strain energy. The accumulation of considerable nitrogen contents at grain boundaries retards grain growth.

2. Retarded crystallization of the amorphous phase: It has been shown that the stability of the amorphous phase created during MA under the nitrogen gas atmosphere is significant [7]. Thus, the crystallization of this phase is expected to be a slow transformation, which can affect the resultant grain size. In our previous work [7], differential scanning calorimetry results on this alloy showed that the onset crystallization temperature of the amorphous phase is nearly 580 ºC. Nevertheless, the thermal stability of the powders had been assessed in a differential scanning calorimeter under a flowing argon gas atmosphere. The employment of this flowing atmosphere gives rise to the removal of nitrogen atoms from the alloy,

This is the accepted manuscript (postprint) of the following article:
E. Salahinejad, R. Amini, M. Marasi, M. J. Hadianfard, *Microstructure and wear behavior of a porous nanocrystalline nickel-free austenitic stainless steel developed by powder metallurgy*, Materials and Design 31 (2010) 2259–2263.
http://dx.doi.org/10.1016/j.matdes.2009.10.008

decreasing the nitrogen concentration in the alloy. However, the application of the encapsulation technique results in the insulation of the samples in a small closed volume, thereby preserving nitrogen in the specimens. On the other hand, it has been proved that the thermal stability of the amorphous phase increases by increasing nitrogen content [7]. Hence, it is expected that during the employed sintering procedure, the thermal stability of the amorphous phase is more than that obtained from the differential scanning calorimetry results.

3.2. Hardness and dry sliding wear

Bulk hardness of the non-porous 316L austenitic stainless steel was measured as 190 Hv. The micro-hardness of the sintered material at pore-free zones was found to be a considerable value of 350 Hv; nonetheless, the bulk hardness which is affected by the pores is 140 Hv. The considerable micro-hardness is justified as below. It is well established that nanostructured materials exhibit higher hardnesses compared to coarse-grained materials, as expected from the Hall-Petch equation [5]. Moreover, it has been found that the nitrogen addition to austenitic stainless steels enhances their hardness. Nitrogen in austenitic stainless steels is an effective element not only in solid-solution strengthening but also in grain size strengthening [21]. In other words, the nitrogen addition to austenitic stainless steels increases both the friction stress and Hall-Petch slope.

The variation of friction coefficient with sliding distance for the porous stainless steel sample slid to 800 m is presented in Fig. 4. As it is obvious, at the low sliding distances the friction coefficient is as small as 0.2 and its value is also fluctuating in a narrow range. Then, a gradual increase in the friction coefficient coupled with fluctuating in a relatively wide

This is the accepted manuscript (postprint) of the following article:
E. Salahinejad, R. Amini, M. Marasi, M. J. Hadianfard, *Microstructure and wear behavior of a porous nanocrystalline nickel-free austenitic stainless steel developed by powder metallurgy*, Materials and Design 31 (2010) 2259–2263.
http://dx.doi.org/10.1016/j.matdes.2009.10.008

range is observable. This increase is due to an increase in the roughness of the contact surface of the sample and the pin tip. Regarding the effect of pores on wear characteristics, it has been reported that porosities in lubricant conditions, such as human body, act as a reservoir of fluids, thereby decreasing the friction coefficient and material wear [17]. It is inferred that in dry conditions, the presence of porosities decreases the contact surface, decreasing the friction coefficient.

Table 2 lists the weight loss of the samples and corresponding pins after sliding to 200, 400, 600, and 800 m. As expected, an increase in the weight loss of the 316L samples and the pins by increasing the sliding distance can be seen. It is also realized that the difference between the weight losses of the 316L samples decreases slightly by increasing the sliding distance, being a consequence of work hardening. The pins also show this behavior. Furthermore, it is observed that the weight loss of the porous specimens is less than that of the 316L samples and does not follow a distinct trend. This can be due to the following contributions:

i) Significant intrinsic hardness of the material (without considering pores): It is well known that the wear resistance of a material is proportional to its hardness [22]. Since the nanostructured high-nitrogen stainless steel has a considerable micro-hardness of up to 350 Hv, it is expected that the material has a substantial inherent resistance against wear.

ii) Specific configuration of pores: It has been reported that when the volume percentage of porosities and the pore size are larger than 7 to 10 % and 12 μm, respectively, the pores behave as a reservoir of wear debris [22,23]. This increases the wear resistance of the specimens by increasing the real contact area and consequently decreasing the contact pressure. Additionally, it has been found that the small wear debris would be trapped inside

This is the accepted manuscript (postprint) of the following article:
E. Salahinejad, R. Amini, M. Marasi, M. J. Hadianfard, *Microstructure and wear behavior of a porous nanocrystalline nickel-free austenitic stainless steel developed by powder metallurgy*, Materials and Design 31 (2010) 2259–2263.
http://dx.doi.org/10.1016/j.matdes.2009.10.008

open pores on the sliding surface, contributing to differences between the wear rate obtained from the depth and weight losses [22,23]. If the trapped debris is not taken out from the porosities before weighing, a smaller weight loss is measured than real values. In addition, it should be considered that the wear debris of the pins can be trapped inside the pores, i.e., a mass gain to the worn samples is also possible. As indicated in Fig. 1, a number of pores are larger than 12 μm in size and also the amount of porosity is nearly 15 vol.%. Therefore, the influence of the pores on the wear behavior is another reason for the small weight loss of the fabricated samples.

Fig. 5 illustrates the SEM micrograph of the worn surface of the porous high-nitrogen specimen after 800 m sliding distance. Fig. 5a displays the general configuration of the worn surface; however, it is noticeable in the higher magnification image (Fig. 5b) that the dominated wear mechanism has been delamination. In the delamination mechanism, the surface layers of the sample are plastically deformed. This localized unidirectional shearing of the alloy surface gives rise to the nucleation of some subsurface voids. These voids extend and link to each other by increasing the deformation of the surface layers, thereby creating some subsurface cracks along the direction of sliding. The growth of these cracks contributes to the collapse of the adhesion of the surface layer to subsurface layers. This leads to the delamination of the deformed surface layer and the generation of flake-like wear particles [23,24].

By considering the worn surface and the insignificant weight wear loss of the porous sample simultaneously, this assumption is supported that the wear debris of both the sample and pin has been trapped inside open pores. Consequently, the material has exhibited the insignificant weight wear loss, as tabulated in Table 2. The XRD pattern of the worn surfaces

This is the accepted manuscript (postprint) of the following article:
E. Salahinejad, R. Amini, M. Marasi, M. J. Hadianfard, *Microstructure and wear behavior of a porous nanocrystalline nickel-free austenitic stainless steel developed by powder metallurgy*, Materials and Design 31 (2010) 2259–2263.
http://dx.doi.org/10.1016/j.matdes.2009.10.008

of the high-nitrogen specimens reveals that no austenite to martensite transformation and no considerable grain growth have occurred during the wear experiments (the related XRD pattern is not presented here). This suggests the high stability of the nanostructured γ phase stabilized by nitrogen.

4. Conclusions

In this work, the structure and dry sliding wear behavior of a nanocrystalline 18Cr–8Mn–0.9N austenitic stainless steel produced by powder metallurgy were considered. Amorphous/nanocrystalline powder synthesized by MA was employed as the primary material. The outcome of this research can be summarized as follows:

1) Low-temperature sintering at 1100 ºC for 20 h and subsequently water-quenching resulted in the development of a nanocrystalline austenitic stainless steel with a relative density of 85%.

2) The sluggish grain growth despite the relatively long sintering time was essentially attributed to the segregation of nitrogen atoms toward grain boundaries and the retarded crystallization of the amorphous phase.

3) The micro-hardness of the sintered samples on pore-free zones was measured as up to 350 Hv, due to the high nitrogen concentration and the nano scale structure.

4) The fabricated porous specimens exhibited insignificant weight wear losses compared with the 316L samples. It was attributed to the high inherent hardness and the specific configuration of pores.

5) The SEM observations on the worn surfaces of the porous samples signified that the dominated wear mechanism has been delamination.

This is the accepted manuscript (postprint) of the following article:
E. Salahinejad, R. Amini, M. Marasi, M. J. Hadianfard, *Microstructure and wear behavior of a porous nanocrystalline nickel-free austenitic stainless steel developed by powder metallurgy*, Materials and Design 31 (2010) 2259–2263.
http://dx.doi.org/10.1016/j.matdes.2009.10.008

Acknowledgements

The authors would like to express their thanks to Shiraz University and Nanyang Technological University (NTU) for their support to this study.

References

[1] Sumita M, Hanawa T, Teoh SH. Development of nitrogen-containing nickel-free austenitic stainless steels for metallic biomaterials-review. Mater Sci Eng C. 2004;24:753-60.

[2] Alvarez K, Sato K, Hyun SK, Nakajima H. Fabrication and properties of lotus type porous nickel-free stainless steel for biomedical applications. Mater Sci Eng C 2008;28:44-50.

[3] Menzel J, Kirschner W, Stein G. High nitrogen containing Ni-free austenitic steels for medical applications. ISIJ Int 1996;36:893-900.

[4] Uggowitzer PJ, Magdowski R, Speidel MO. Nickel free high nitrogen austenitic steels. ISIJ Int 1996;36:901-08.

[5] Benson D, Meyers MA, Mishra A. Mechanical properties of nanocrystalline materials. Prog Mater Sc. 2006;51:427-56.

[6] Suryanarayana C. Mechanical alloying and milling. Prog Mater Sci 2001;46:1-184. [7] Amini R, Hadianfard MJ, Salahinejad E, Marasi M, Sritharan T. Microstructural phase evaluation of high-nitrogen Fe–Cr–Mn alloy powders synthesized by the mechanical alloying process. J Mater Sci 2009;44:136-48.

[8] Amini R, Shokrollahi H, Salahinejad E, Hadianfard MJ, Marasi M, Sritharan T. Microstructural, thermal and magnetic properties of amorphous/nanocrystalline FeCrMnN

alloys prepared by mechanical alloying and subsequent heat treatment. J Alloys Compd 2009;480:617-24.

[9] Salahinejad E, Amini R, Marasi M, Sritharan T, Hadianfard MJ. The effect of nitrogen on the glass-forming ability and micro-hardness of Fe–Cr–Mn–N amorphous alloys prepared by mechanical alloying. Mater Chem Phys 2009; doi: 10.1016/j.matchemphys.2009.07.005.

[10] Salahinejad E, Amini R, Marasi M, Hadianfard MJ. The effect of sintering time on the densification and mechanical properties of a mechanically alloyed Cr–Mn–N stainless steel. Mater Des 2010;31:527–32.

[11] Cisneros MM, Lopez HF, Mancha H, Vazquez D, Valdes E, Mendoza G, Mendez M. Development of austenitic nanostructures in high-nitrogen steel powders processed by mechanical alloying. Metall Mater Trans A 2002;33:2139-44.

[12] Mendez M, Mancha H, Cisneros MM, Mendoza G, Escalante JI, Lopez HF. Structure of a Fe–Cr–Mn–Mo–N alloy processed by mechanical alloying. Metall Mater Trans A 2002;33:3273-8.

[13] Cisneros MM, Lopez HF, Mancha H, Rincon E, Vazquez D, Perez MJ, Torre SDDL. Processing of nanostructured high nitrogen stainless steel by mechanical alloying. Metall Mater Trans A 2005;36:1309-16.

[14] Dewidar MM, Khalil KA, Lim JK. Processing and mechanical properties of porous 316L stainless steel for biomedical applications. Trans Nonferrous Me. Soc China 2007;17:468-73.

[15] Cui D, Jiang J, Cao G, Xiao E, Qu X. Preparation of high nitrogen and nickel-free austenitic stainless steel by powder injection molding. J Univ Sci Technol Beijing 2008;15:150-4.

This is the accepted manuscript (postprint) of the following article:
E. Salahinejad, R. Amini, M. Marasi, M. J. Hadianfard, *Microstructure and wear behavior of a porous nanocrystalline nickel-free austenitic stainless steel developed by powder metallurgy*, Materials and Design 31 (2010) 2259–2263.
http://dx.doi.org/10.1016/j.matdes.2009.10.008

[16] Thomann UI, Uggowitzer PJ. Wear-corrosion behavior of biocompatible austenitic stainless steels. Wear 2000;239:48-58.

[17] Gradzka-Dahlke M, Dabrowski JR, Dabrowski B. Characteristic of the porous 316 stainless steel for the friction element of prosthetic joint. Wear 2007;263:1023-9.

[18] Saravanan P, Raja VS, Mukherjee S. Effect of plasma immersion ion implantation of nitrogen on the wear and corrosion behavior of 316LVM stainless steel. Surf Coat Technol 2007;201:8131-5.

[19] Li CX, Bell T. Sliding wear properties of active screen plasma nitride 316 austenitic stainless steel. Wear 2004;256:1144-52.

[20] Manova D, Hirsch D, Richter E, Mändl S, Neumann H, Rauschenbach B. Microstructure of nitrogen implanted stainless steel after wear experiment. Surf Coat Technol 2007;201:8329-33.

[21] Simmons JW. Overview: High-nitrogen alloying of stainless steels. Mater Sci Eng A. 1996;207:159-69.

[22] Kameo K, Nishiyabu K, Friedrich K, Tanaka S, Tanimoto T. Sliding wear behavior of stainless steel parts made by metal injection molding (MIM). Wear 2006;260:674-86.

[23] Gulsoy HO. Dry sliding wear in injection molded 17-4 PH stainless steel powder with nickel boride additions. Wear 2007;262:491-7.

[24] Lim SC, Ashby MF. Wear-mechanism maps. Acta Metal 1987;35:l-24.

This is the accepted manuscript (postprint) of the following article:
E. Salahinejad, R. Amini, M. Marasi, M. J. Hadianfard, *Microstructure and wear behavior of a porous nanocrystalline nickel-free austenitic stainless steel developed by powder metallurgy*, Materials and Design 31 (2010) 2259–2263.
http://dx.doi.org/10.1016/j.matdes.2009.10.008

Figures:

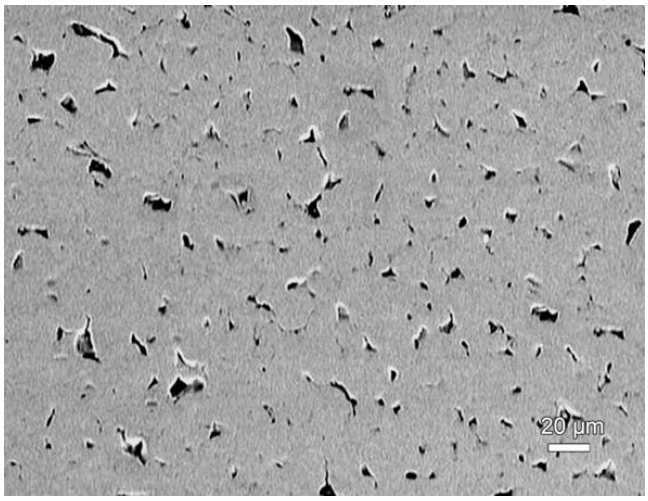

Fig. 1. SEM micrograph of the specimen sintered at 1100 ºC for 20 h.

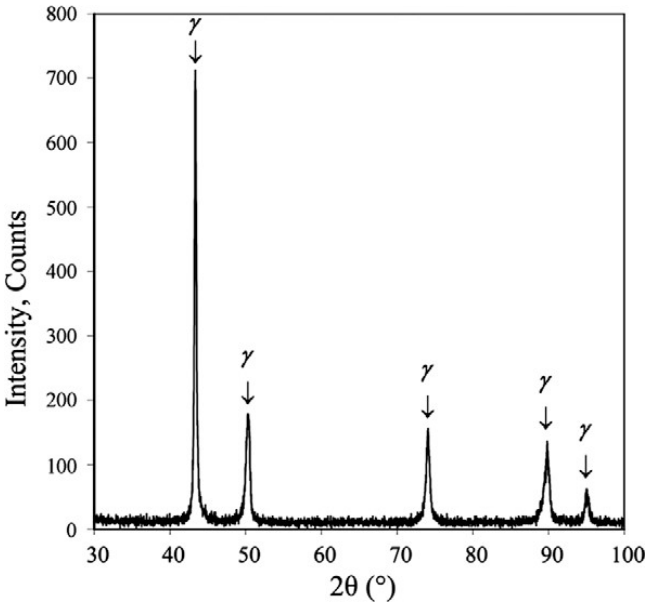

Fig. 2. XRD trace of the sample sintered at 1100 ºC for 20 h and water-quenched.

This is the accepted manuscript (postprint) of the following article:
E. Salahinejad, R. Amini, M. Marasi, M. J. Hadianfard, *Microstructure and wear behavior of a porous nanocrystalline nickel-free austenitic stainless steel developed by powder metallurgy*, Materials and Design 31 (2010) 2259–2263.
http://dx.doi.org/10.1016/j.matdes.2009.10.008

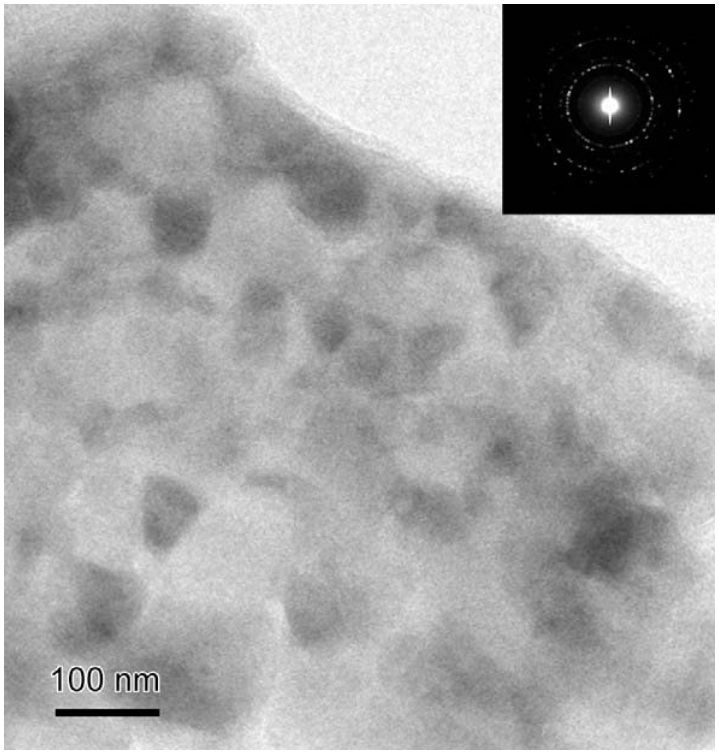

Fig. 3. TEM image and corresponding SAD pattern of the sintered material.

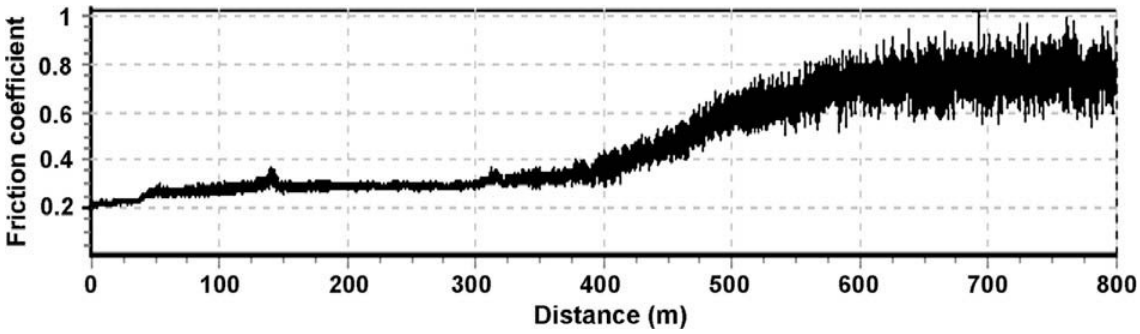

Fig. 4. Friction coefficient with sliding distance for the nickel-free stainless steel sample slid to 800 m.

This is the accepted manuscript (postprint) of the following article:
E. Salahinejad, R. Amini, M. Marasi, M. J. Hadianfard, *Microstructure and wear behavior of a porous nanocrystalline nickel-free austenitic stainless steel developed by powder metallurgy*, Materials and Design 31 (2010) 2259–2263.
http://dx.doi.org/10.1016/j.matdes.2009.10.008

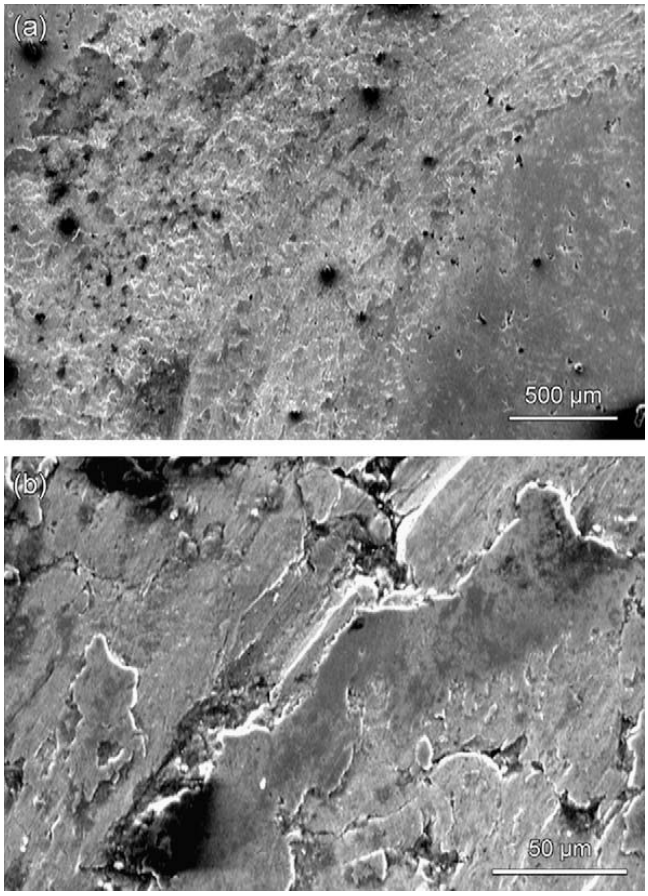

Fig. 5. SEM picture of the worn surface of the nickel-free stainless steel sample after 800 m sliding distance in two magnifications.

This is the accepted manuscript (postprint) of the following article:
E. Salahinejad, R. Amini, M. Marasi, M. J. Hadianfard, *Microstructure and wear behavior of a porous nanocrystalline nickel-free austenitic stainless steel developed by powder metallurgy*, Materials and Design 31 (2010) 2259–2263.
http://dx.doi.org/10.1016/j.matdes.2009.10.008

Tables:

Table 1. Chemical composition of the nickel-free stainless steel powder (wt.%)

Fe	Cr	Mn	N	O	C
72.948	17.643	8.069	0.973	0.334	0. 033

Table 2. Weight loss of the specimens and the corresponding pins

Sliding distance (m)	Weight loss (mg)			
	The porous stainless steel	The 316L stainless steel	The pins of the porous sample	The pins of the 316L sample
200	0.1 <0.1>	3.2 <0.2>	0.3 <0.1>	0.2 <0.1>
400	0 <0.1>	6.9 <0.1>	0.9 <0.2>	0.6 <0.4>
600	0.2 <0.2>	8.6 <0.3>	1.4 <0.3>	0.9 <0.3>
800	0.2 <0.1>	9.1 <0.2>	1.8 <0.4>	1.1 <0.3>

Error value: $<X> = \pm X$